Int. J. Heat Mass Transfer. Vol. 23, pp. 1505–1519

0017-9310/80/1101-1505 $02.00/0

HEAT TRANSFER BETWEEN A HORIZONTAL TUBE AND A GAS–SOLID FLUIDIZED BED

N. S. GREWAL* and S. C. SAXENA

Department of Energy Engineering, University of Illinois at Chicago Circle, Box 4348, Chicago, IL 60680, U.S.A.

(*Received* 31 *August* 1979 *and in revised form* 14 *March* 1980)

Abstract — Experiments have been conducted to measure the heat transfer coefficient between an electrically heated single horizontal tube and air–solid fluidized beds of glass beads, dolomite, sand, silicon carbide and alumina particles. The effect of size, shape and density of the particle, specific heat, air mass fluidizing velocity, tube size, tube material, bed depth, heat flux and distributor design on heat transfer rate has been investigated. Experimental results of heat transfer coefficient, h_w, are compared with the predictions of the existing correlations for these quantities. These correlations are found to be inadequate to reproduce the present data. Therefore a correlation has been proposed for h_w on the basis of our experimental data and examined to assess its appropriateness on the basis of available data in the literature.

NOMENCLATURE

A, cross sectional area of bed, m^2;
A_w, surface area of a smooth tube, m^2;
C_{pf}, specific heat of fluidizing air at constant pressure, $kJ\,kg^{-1}\,K^{-1}$;
C_{ps}, specific heat of solid particles, $kJ\,kg^{-1}\,K^{-1}$;
$\bar{d}_p$, average particle diameter defined by equation (1), m;
d_{pi}, arithmetic average diameter of the successive screens, m;
D_b, bed diameter, m;
D_T, outside diameter of a smooth heat transfer tube, m;
$D_{12.7}$, heat transfer tube 12.7 mm in diameter, m;
g, acceleration due to gravity, $m\,s^{-2}$;
G, superficial mass fluidizing velocity, $kg\,m^{-2}\,s^{-1}$;
G_{mf}, mass velocity at minimum fluidizing condition, $kg\,m^{-2}\,s^{-1}$;
h_w, total average heat transfer coefficient for a smooth tube, $W\,m^{-2}\,K^{-1}$;
H, distance between pressure probes, m;
H_{mf}, bed height at minimum fluidizing condition, m;
H_s, static bed height, m;
k_f, thermal conductivity of air, $W\,m^{-1}\,K^{-1}$;
Nu_{wp}, Nusselt number based on particle diameter, $=(h_w\bar{d}_p)/k_f$, dimensionless;
Nu_{wT}, Nusselt number based on tube diameter, $=(h_wD_T)/k_f$, dimensionless;
Q, electrical power supplied to heater, W;
Pr, Prandtl number, $=(\mu C_{pf})/k_f$, dimensionless;
Re_p, Reynolds number, $=(G\bar{d}_p/\mu)$, dimensionless;
T_b, average fluidized bed temperature, K;
T_w, average surface temperature of the heat transfer tube, K;
U, superficial fluidizing velocity, $m\,s^{-1}$;
U_{mf}, minimum fluidizing velocity, $m\,s^{-1}$;
w_i, weight fraction of particles in a specified size range, dimensionless;
W, weight of the bed, kg.

Greek letters

ΔP, pressure drop across the probes, Pa;
ε, bulk bed porosity, dimensionless;
ε_{mf}, bulk bed porosity at minimum fluidizing condition, dimensionless;
$1-\varepsilon$, volume fraction of bed occupied by particles, dimensionless;
ρ_f, fluidizing gas density, $kg\,m^{-3}$;
ρ_s, density of solid particles, $kg\,m^{-3}$;
μ, viscosity of the fluidizing gas $Ns\,m^{-3}$;
ϕ_s, sphericity of solid particles, dimensionless.

1. INTRODUCTION

THE RECENT energy crisis has given added incentive to the development of efficient techniques for power generation by the use of available fossil fuels in the United States. One such fuel is coal and extensive work is going on to develop fluidized-bed combustion of coal to generate steam and compressed hot gases to drive turbines in a combined power cycle. The bed has imbedded boiler tubes through which water is passed to generate steam. An efficient design requires the knowledge of the heat transfer coefficient between the tube and the bed, and its dependence on operating conditions, bed material and tube dimensions. The present experimental effort is motivated to produce information to achieve this final goal. In particular, we report data for the average heat transfer coefficient for a horizontal tube (electrically heated) immersed in a fluidized bed of particles (less than 1 mm) of different properties at room temperature as a function of fluidizing velocity. The fluidized-bed combustors

*Present address: Department of Mechanical Engineering, University of North Dakota, Grand Forks, ND 58202, U.S.A.

burning high sulfur coal in a bed of limestone or dolomite use larger particles, greater than 1 mm. However, the information reported here will be directly useful for the design of low rank coal fluidized bed combustors. Here, crushed low rank coal is burnt in inert bed of silica sand or alumina particles of size less than 1 mm. A pilot plant to study the combustion characteristics of low rank coals is in operation at the Grand Forks Energy Technology Center [1].

There are a number of exhaustive reviews of basic studies on fluidized bed heat transfer [1–10]. The majority of the experimental and theoretical effort has been toward an understanding of the mechanisms of heat transfer to fluidized beds by unsteady-state conduction to moving solid particles at temperatures such that radiation can be neglected (<900 K) and with particle sizes (<1 mm) sufficiently small so that gas convection can also be neglected for nonpressurized systems. Based on the analysis of the existing studies of mechanisms of wall-to-bed heat transfer, Saxena *et al.* [10] have suggested the various factors which must be considered in developing a generalized correlation. These are: (a) the principal mode of heat removal is by fluidized-particle heat absorption and therefore the volumetric heat capacity of the particles must be considered; (b) heat is conducted from the wall and between the absorbing particles through the interstitial gas phase and therefore a generalized correlation must contain gas thermal conductivity; and (c) the rate of heat transfer depends on the particle residence time and therefore a generalized correlation should account for at least the bubbling characteristics, particle drag forces and the system geometry.

A number of experimental investigations have been reported on the measurement of heat transfer rate between a horizontal tube and fluidized beds [10–37]. Several correlations have been proposed for the total average heat transfer coefficient, h_w, and these are listed in Table 1. These correlations have been employed for the interpretation of our experimental data.

None of the correlations for h_w include all the important parameters mentioned above. The purpose of this paper is two-fold. First, to check the validity of the existing correlations by comparing them with our data obtained for different particle sizes and shapes, particle physical and thermal properties, tube sizes, tube materials and operating conditions. Secondly, to propose a new general correlation involving volumetric heat capacity of solid particles and such other important parameters which have not been included in earlier works. The proposed correlation is also assessed on the basis of available data in the literature.

2. EXPERIMENTAL APPARATUS AND PROCEDURE

The details of the fluidized bed system employed in the present series of experiments are given in our earlier publications [1, 35, 37]. It is instrumented for the measurement of temperature, pressure, air flow rate, and power supplied to the heat transfer tubes. The fluidizing column (30.5 × 30.5 cm) is supplied with air which flows through an air jet breaker plate in the calming section and then through the fluidized bed distributor plate. The heat transfer tube is mounted

Table 1. Different correlations for the prediction of the total heat transfer coefficient, h_w

Reference	Correlations
Vreedenberg [11]	$Nu_{wT} = 420\left[\left(\frac{GD_T\rho_s}{\rho_f\mu}\right)\left(\frac{\mu^2}{\bar{d}_p^3\rho_s^2 g}\right)\right]^{0.3} Pr^{0.3}$
Andeen and Glicksman [15]	$Nu_{wT} = 900(1-\varepsilon)\left[\left(\frac{GD_T\rho_s}{\rho_f\mu}\right)\left(\frac{\mu^2}{\bar{d}_p^3\rho_s^2 g}\right)\right]^{0.326} Pr^{0.3}$
Petrie *et al.* [13]	$Nu_{wT} = 14(G/G_{mf})^{1/3} Pr^{1/3}(D_T/\bar{d}_p)^{2/3}$
Ainshtein [14]	$Nu_{wT} = 5.76(1-\varepsilon)\left(\frac{Gd_p}{\mu\varepsilon}\right)^{0.34} Pr^{0.33}(H_s/D_b)^{0.16}(D_T/\bar{d}_p)$
Gelperin *et al.* [16]	$Nu_{wT} = 4.38\left[\frac{1}{6(1-\varepsilon)}\left(\frac{G\bar{d}_p}{\mu}\right)\right]^{0.32}\left(\frac{1-\varepsilon}{\varepsilon}\right)(D_T/\bar{d}_p)$
Genetti *et al.* [17]	$Nu_{wT} = \frac{11(1-\varepsilon)^{0.5}}{1+\left[\frac{0.2512}{\left(\frac{G\bar{d}_p}{\mu}\right)^{0.24}(\bar{d}_p/0.000203)^2}\right]^2}(D_T/\bar{d}_p)$
Ternovskaya and Korenberg [12]	$Nu_{wT} = 2.9\left[\left(\frac{1-\varepsilon}{\varepsilon}\right)\left(\frac{G\bar{d}_p}{\mu}\right)\right]^{0.4} Pr^{0.33}(D_T/\bar{d}_p)$

Table 2. Minimum fluidization velocity and relevant properties of solid particles

Material	$\bar{d}_p$ (μm)	ρ_s (kg m^{-3})	G_{mf} (kg m^{-2} s^{-1})	C_{ps} (kJ kg^{-1} K^{-1})	ε_{mf}	ϕ_s	H_{mf} (cm)
Silicon	178	3220	0.047	0.837	0.495	0.67	31.1
Carbide	362	3240	0.187	0.837	0.49	0.67	36.8
Alumina	259	4015	0.125	0.766	0.51	0.64	34.7
Silica	167	2670	0.0325	0.800	0.44	0.81	35.8
	451	2670	0.181	0.800	0.41	0.84	33.7
	504	2670	0.264	0.800	0.42	0.88	36.2
Dolomite	293	2840	0.126	0.929	0.525	0.635	23.7
Glass beads	265	2490	0.071	0.754	0.40	1.00	36.0
	357	2490	0.127	0.754	0.40	1.00	35.7
	427	2490	0.1955	0.754	0.405	1.00	36.7
Lead glass	241	4450	0.1115	0.440	0.40	1.00	36.0
Dolomite	312	2840	0.1415	0.929	0.54	0.60	26.6

horizontally with its center axis 213 mm above the distributor plate. Three different distributor plates employed in the present work consist of two perforated plates with an open area of 37.5 and 7.7% [37], and a bubble cap distributor with an open area of 0.2% [36].

The fluidizing air is supplied by a compressor and its flow rate is measured on calibrated rotameters with an accuracy of $\pm 1\%$. The pressure in the fluidized bed at various locations is measured with manometers. The heat transfer tube is electrically heated with a calrod heater, and is fitted with eight iron–constantan thermocouples. The ends of the tubes are provided with Teflon support to reduce axial heat loss which is estimated to be less than 1%. A DC power supply with a voltage regulation of $\pm 0.01\%$ is used to energize the heater. A voltmeter and an ammeter with an accuracy of $\pm 0.5\%$ are used to measure the electric power supplied to the heater. Two thermocouples are used to measure the fluidized-bed temperature and these are located 13.3 cm above and below the heat transfer tube. The average of these two values is used in the calculation of the heat transfer coefficient. In our experiments for $G/G_{mf} > 1.3$, the difference between the temperature indicated by the two thermocouples never exceeded 0.16 K (0.3 °F). The top thermocouple readings are always greater than the bottom thermocouple. The average temperature difference between the tube surface and the bed varies between 10 and 35 K depending on particle size, fluidizing velocity and tube size. The thermocouples are connected to a Leeds and Northrup Numatron temperature recorder with 0.1 K resolution and a 21 column digital printer.

Minimum fluidizing velocity and relevant physical and thermal properties of the solid particles used in the present investigations are reported in Table 2. The average diameter of particles, $\bar{d}_p$, is obtained from the sieve analysis of solid particles and using the following relation:

$$\bar{d}_p = \frac{1}{\sum_i (w/d_p)_i}. \tag{1}$$

The minimum fluidizing velocity for a given bed of solid particles is determined in the conventional fashion [7] by measuring the pressure drop as a function of fluidizing velocity. The minimum fluidizing velocity is established by the intersection of the two linear plots describing the constant and decreasing pressure drop with decreasing fluidizing velocity [38].

The values of ε_{mf} are calculated from the following simple relation:

$$\frac{W}{AH_{mf}} = (1 - \varepsilon_{mf})(\rho_s - \rho_f)g. \tag{2}$$

The sphericity of solid particles, ϕ_s, is obtained by using the Ergun correlation [7],

$$\frac{1.75(\phi_s \bar{d}_p)}{\mu \rho_f \varepsilon_{mf}^3} G_{mf}^2 + 150\left(\frac{1 - \varepsilon_{mf}}{\varepsilon_{mf}^3 \rho_f}\right) G_{mf} = \frac{(\phi_s \bar{d}_p)^2 (\rho_s - \rho_f) g}{\mu}. \tag{3}$$

The calculated values of ε_{mf} and ϕ_s are listed in Table 2.

The settled or slumped bed height is kept the same in all experiments at approximately 35 cm. A typical experiment involves recording the surface temperature of the tube using eight thermocouples located at various positions, bed temperature and inlet air temperature. The steady state in heat transfer experiments is assumed to be established when the time-averaged bed temperature variation is less than 0.2 K h^{-1}. The following equation is used to calculate the average heat transfer coefficient, h_w,

$$h_w = \frac{Q}{A_w(T_w - T_b)}. \tag{4}$$

The maximum absolute error in experimental values of h_w is estimated as $\pm 8\%$. The precision of our measurements as judged from the reproducibility of the data points is about 2%.

The pressure loss in a fluidized bed, ΔP, is equal to the weight of the bed per unit cross-sectional area i.e.,

$$\Delta P = H(1 - \varepsilon)(\rho_s - \rho_f). \tag{5}$$

The above relation is used to measure the average bed porosity in the vicinity of the heat transfer tube by measuring the bed pressure drop, ΔP, between the two pressure probes mounted flush with the column wall and 13.3 cm above and below the center of the heat

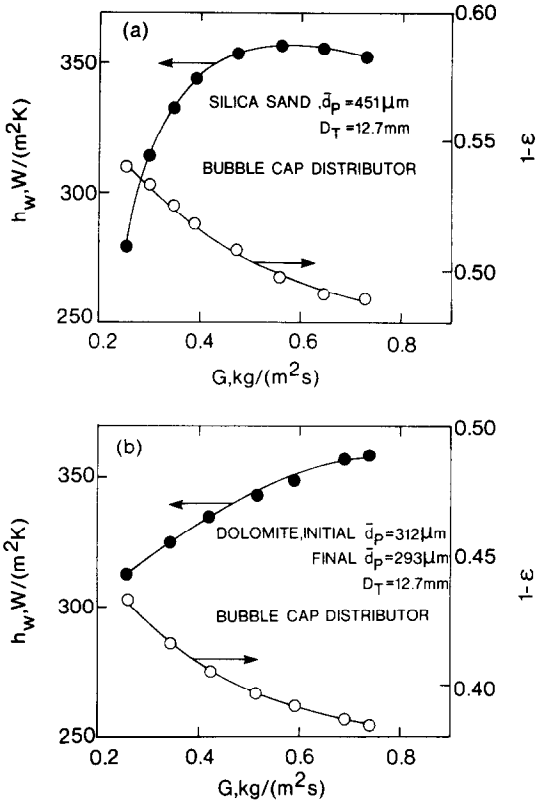

FIG. 1. Average heat transfer coefficient as a function of mass fluidizing velocity.

transfer tube. The fluctuation in ΔP is observed to be a function of $G - G_{mf}$, bed material and distributor design. The pressure drop across the bed is recorded over a period of time and an average value is employed in equation (5) to calculate ε.

3. EXPERIMENTAL RESULTS

Experimental values of the average heat transfer coefficient, h_w, and particle fraction in the bed, $1 - \varepsilon$, are shown in Figs. 1–7. The qualitative variation of the dependence of h_w on G in each case is in complete agreement with the reported trends observed by various earlier investigators [3, 5]. The values of h_w increase with an increase in the value of G, but decrease with larger gas velocities and attains a maximum at some intermediate value (Figs. 1 and 6). This can be explained on the basis of the "particle mode" of heat transfer [39] and known concepts involving the particle residence time on the surface and particle density close to the surface. The magnitude of h_w depends upon the net contribution arising from these two opposing factors.

The heat transfer coefficient decreases with an increase in solid particle diameter as seen from Figs. 2(b), 4(a) and 5. This qualitative trend is in complete agreement with the reported findings in the literature [3, 5, 35, 36]. The decrease in h_w with an increase in particle diameter ($\bar{d}_p < 1$ mm) is explained as predominantly due to an increase in the average gas

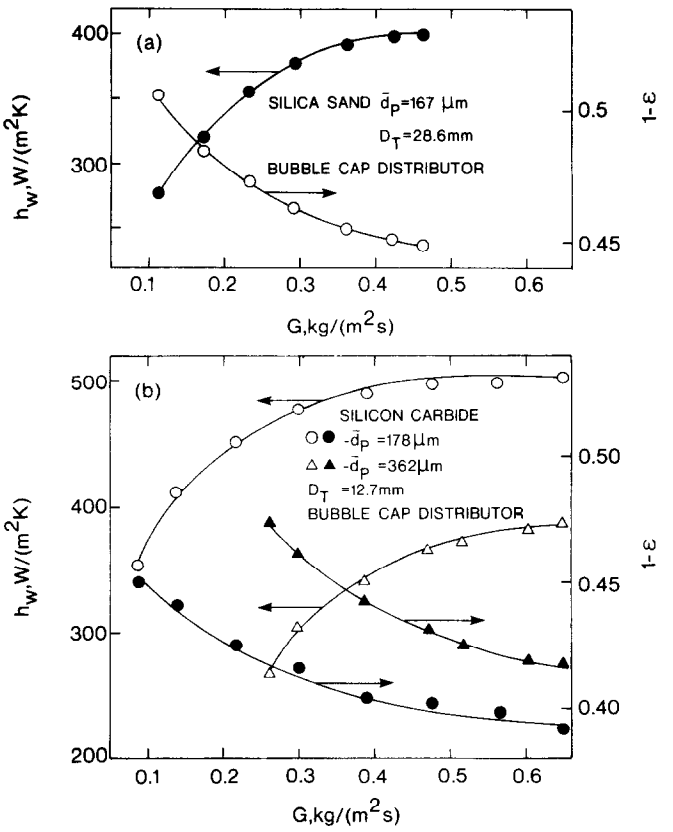

FIG. 2. Average heat transfer coefficient as a function of mass fluidizing velocity.

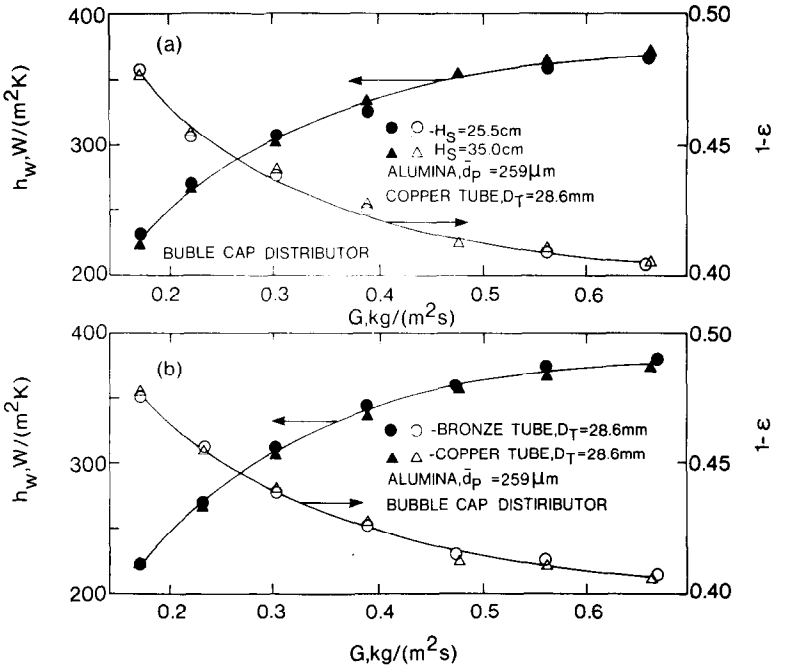

FIG. 3. Average heat transfer coefficient as a function of mass fluidizing velocity.

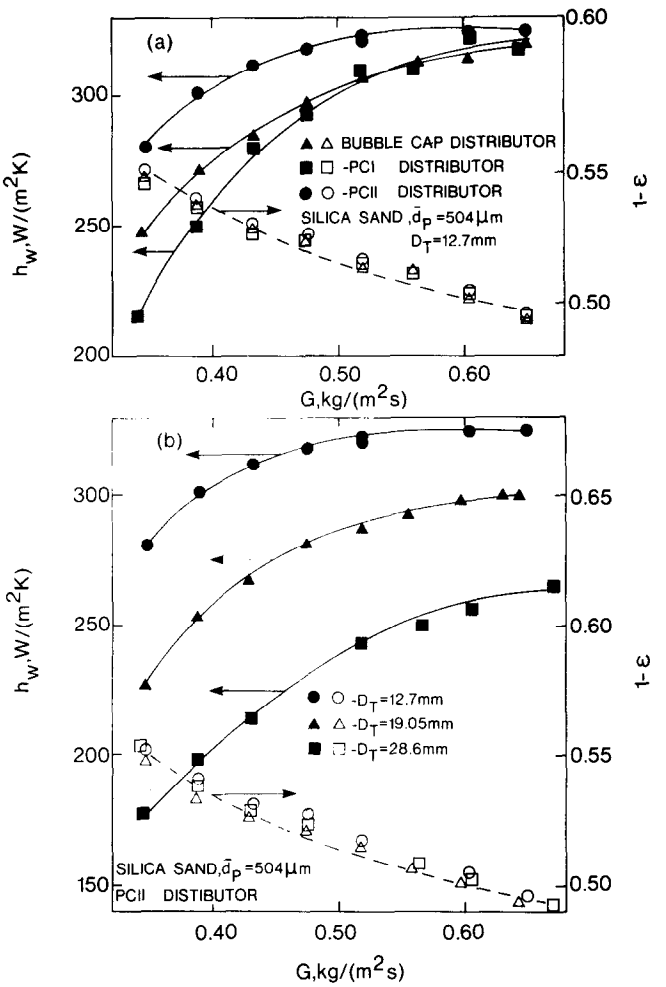

FIG. 4. Average heat transfer coefficient as a function of mass fluidizing velocity

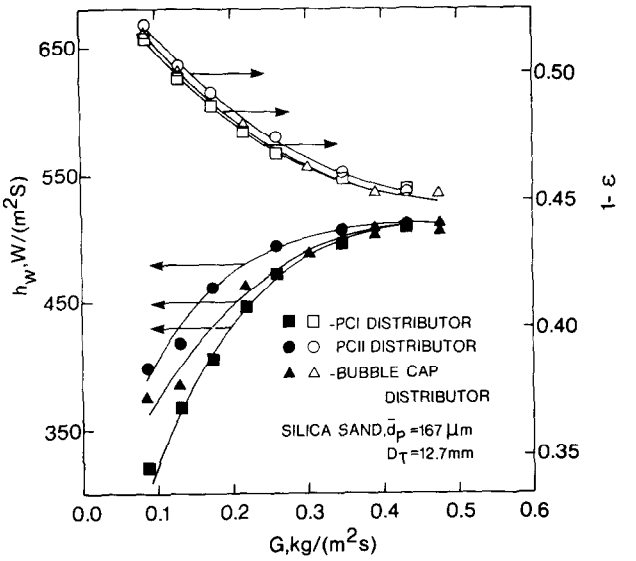

FIG. 5. Average heat transfer coefficient as a function of mass fluidizing velocity.

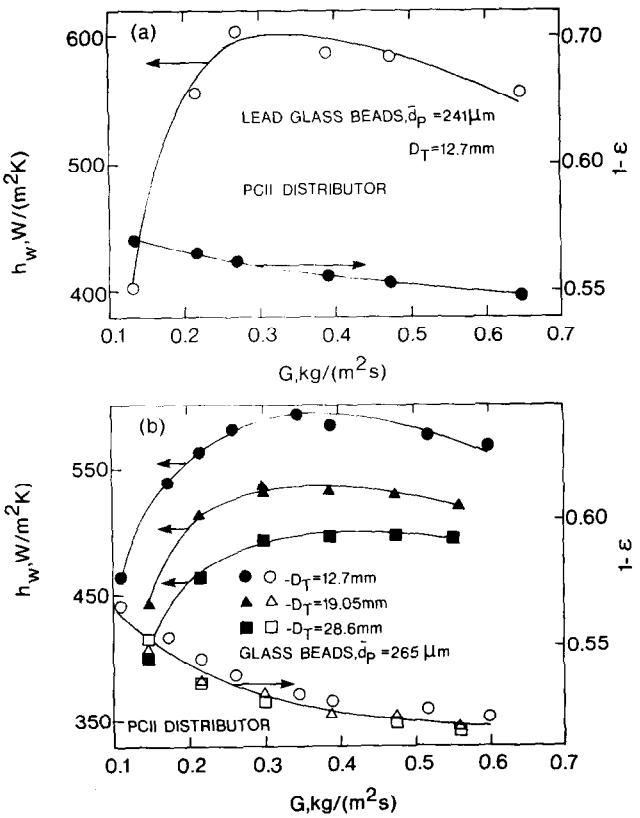

FIG. 6. Average heat transfer coefficient as a function of mass fluidizing velocity.

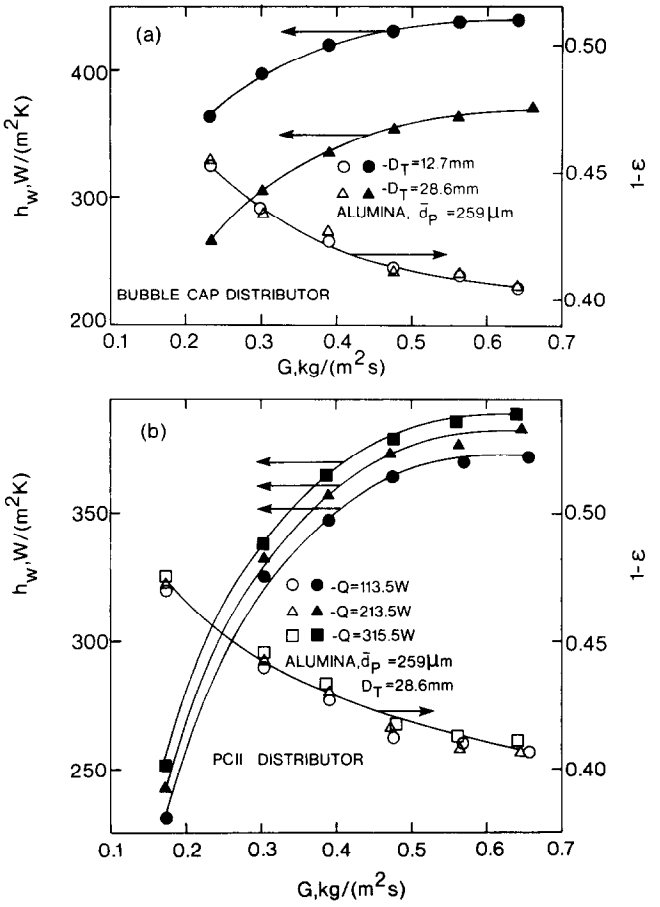

FIG. 7. Average heat transfer coefficient as a function of mass fluidizing velocity.

conduction paths between the heat transfer tube and the first row of particles and between particles. The increase in the gas conduction path increases the resistance to heat flow. Further, the particle surface area per unit volume of the bed is larger for small particles and therefore small particles are more efficient in exchanging heat with the surface.

The effect of bed height, H_s, on h_w is displayed in Fig. 5(a). A single curve can be used to represent data for the two bed heights of 25.5 cm and 35.0 cm. Thus, at least in this range practically no influence of bed height on h_w is observed.

The effect of tube material on h_w is demonstrated in Fig. 3(b). The main motivation of these experiments is to check the adequacy of our experimental procedure for the determination of the average surface temperature of the heat transfer tubes of different materials employed in the present work. It is evident that a single curve can be used to represent the data for copper and bronze tubes within the reproducibility of our experiments. Thus, this result substantiates the adequacy of the adopted procedure for the measurement of average surface temperature of the tube. Further, it may be concluded that, as expected, the tube material does not have any influence on h_w.

The values of the heat transfer coefficient decrease with an increase in tube diameter as shown by Figs. 4(b), 6(b) and 7(a). This is also in agreement with earlier investigations [11, 13, 27]. This decrease is due to an increase in the temperature of the solid particles as they flow around the tube. Under similar fluidizing conditions, the temperature rise of the solid particles will be larger while flowing past the tubes of larger diameter compared with tubes of smaller diameter.

The effect of the distributor design on h_w for the two sizes of silica sand is displayed in Figs. 4(a) and 5. The distributor design influences the values of h_w mainly at low values of G. With increase in the value of G, the difference in values of h_w for different distributors decreases; at the optimum fluidizing velocity, practically identical values of h_w are found. This dependence of h_w on distributor design has already been explained qualitatively on the basis of bubble size and particle mixing in the bed [37].

The effect of heat flux (Q = 113.5–315.5 W) on h_w for alumina ($\bar{d}_p$ = 259 μm) is sketched in Fig. 7(b). It is seen that h_w increases with an increase in heat flux. This is because the thermal conductivity of the fluidizing

medium increases with an increase in bed temperature. A similar conclusion has been derived by Priebe and Genetti [34].

4. AVERAGE HEAT TRANSFER COEFFICIENT

4.1. *Comparison of present experimental values of* h_w *with existing correlations*

The comparison of the present h_w data with seven existing correlations is shown in Figs. 8–14(a). None of these correlations are able to predict values of h_w for all the present experimental conditions. The correlations of Ainshtein [14] and Gelperin *et al.* [16] consistently overpredict h_w. The correlation of Petrie *et al.* [13] gives a good prediction for coarse sand ($\bar{d}_p$ = 451 and 504 μm) but is only reasonably successful for silicon carbide ($\bar{d}_p$ = 362 μm) and glass beads. On the other hand, the predictions for alumina, dolomite, fine sand ($\bar{d}_p$ = 167 μm) and silicon carbide ($\bar{d}_p$ = 178 μm) are rather poor. These general comments are valid for all three sizes of heat transfer tubes (D_T = 12.7–28.6 mm). The correlation of Ternovskaya and Korenberg [12] predicts the data for glass beads better than any other correlation. However, it over-estimates the rest of the present data. The correlation of Genetti *et al.* [17] consistently over-predicts the present data except for glass beads.

Vreedenberg's correlation [11] as modified by Andeen and Glicksman [15] gives good predictions for all heat transfer data, excluding fine sand ($\bar{d}_p$ = 167 μm), for a 12.7 mm diameter tube. With increase in tube diameter, the correlation fails to predict the experimental data both for 19.1 and 28.6 mm diameter heat transfer tubes. Vreedenberg's correlation [11] predicts h_w for sand, alumina and silicon carbide and for 12.7 mm diameter tube as well as modified Vreedenberg's correlation [2]. The predictions for dolomite are not good. From these comments, it is clear that a correlation which can predict all of the present data is needed and this is given in the next section.

4.2. *A proposed correlation*

While the modified Vreedenberg's correlation does include the gas thermal conductivity (k_f), geometry effects (D_T) and terms related to particle drag forces ($\bar{d}_p$, μ, ρ_s), the volumetric heat capacity of solid particle ($\rho_s C_{ps}$) is neglected. The dependence of h_w on $\rho_s C_{ps}$ is well known [3, 39] and has been verified experimentally by Ziegler *et al.* [25, 39]. Therefore, a correlation of the following form is being proposed,

$$Nu_{wT} = c(1-\varepsilon)\left(\frac{GD_T\rho_s}{\rho_f\mu}\frac{\mu^2}{\bar{d}_p^3\rho_s^2 g}\right)^d \cdot\left(\frac{\rho_s C_{ps} D_T^{3/2} g^{1/2}}{k_f}\right)^e Pr^{0.30}, \quad (6)$$

where bulk bed porosity is given by [1]:

$$\varepsilon = \frac{1}{2.1}\left[0.4 + \left\{4\left(\frac{\mu G}{\bar{d}_p^2(\rho_f(\rho_s-\rho_f)\phi_s^2 g)}\right)^{0.43}\right\}^{1/3}\right]. \quad (7)$$

This is of the same form as the modified Vreedenberg's correlation except for an additional dimensionless factor, ($\rho_s C_{ps} D_T^{3/2} g/k_f$), which accounts for the volumetric heat capacity of solid particles, the tube diameter, and the thermal conductivity of the fluidizing gas. The values of the constants c, d and e are obtained by regression analysis of the present data on sand ($\bar{d}_p$ = 451, 504 μm), silicon carbide ($\bar{d}_p$ = 178, 362 μm), alumina ($\bar{d}_p$ = 259 μm) and glass beads ($\bar{d}_p$ = 265, 241 μm) and Ziegler's data [25] on copper, nickel and solder ($\bar{d}_p$ = 136 μm). The final form, the above correlation of equation (6) assumes, is

$$Nu_{wT} = 47(1-\varepsilon)\left(\frac{GD_T\rho_s}{\rho_f\mu}\frac{\mu^2}{\bar{d}_p^3\rho_s^2 g}\right)^{0.325} \cdot\left(\frac{\rho_s C_{ps} D_T^{3/2} g^{1/2}}{k_f}\right)^{0.23} Pr^{0.30}. \quad (8)$$

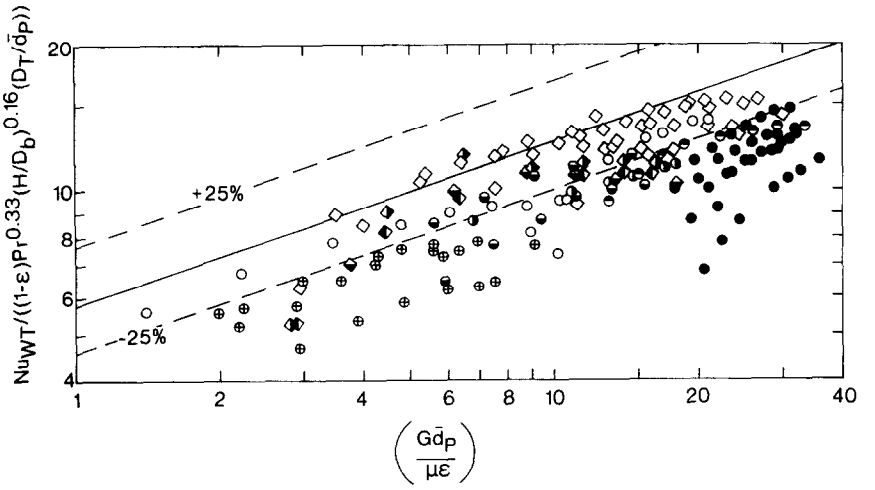

FIG. 8. Comparison of the present experimental data with Ainshtein's correlation [14]. Symbols and other related details are explained in Table 3.

Table 3. Key to Figs. 8–15

Reference	Symbol	Solid particles: Material	Solid particles: $\bar{d}_p$ (μm)	D_T (m)	Bed temperature (K)
Present	○	SiC	178, 362	0.0127	Room temperature
Present	◒	Alumina	259	0.0127, 0.0286	Room temperature
Present	◓	Silica sand	451	0.0127	Room temperature
Present	◑	Dolomite	312	0.0127	Room temperature
Present	●	Silica sand	504	0.0127, 0.0191, 0.0286	Room temperature
Present	⊕	Silica sand	167	0.0127, 0.0286	Room temperature
Grewal *et al.* [37]	◇	Glass beads	265, 357, 427	0.0127	Room temperature
Present	◆	Glass beads	265	0.0191	Room temperature
Present	◆	Glass beads	265	0.0286	Room temperature
Present	◆	Lead-glass beads	241	0.0127	Room temperature
Chen [22]	⊖	Glass beads	240	0.025	Room temperature
Ziegler [25]	□	Nickel	136	0.0127	
	+	Copper	136	0.0127	Room temperature
	◐	Solder	136	0.0127	
Antonshin [26]	△	Quartz sand	268	0.014, 0.021, 0.028	Room temperature
Cherrington *et al.* [32]	◈	Glass beads	390, 1000	0.0508	Room temperature
	◈	Limestone	1000	0.0508	
Howe *et al.* [31]	▲	Dolomite	800	0.0508	1028, Tube bundle
Gelperin *et al.* [29]	▲	Quartz sand	350	0.020	Room temperature
Andeen and Glicksman [15]	◐	Ottawa sand	360, 710	0.0191	Room temperature
Bartel and Genetti [28]	◆	Glass beads	203, 279, 470	0.0159	Room temperature
Gelperin *et al.* [27]	▲	Quartz sand	263	0.020	Room temperature
	▲	Quartz sand	163	0.025	Room temperature
Noack [30]	◆	Glass beads	600	0.025	Room temperature
Natusch and Blenke [20]	◈	Glass beads	450	0.025	Room temperature
Janssen [18]	▼	Quartz sand	1000	0.018	473
Neukirchen and Blenke [33]	◁	Glass beads	500	0.025	Room temperature,
	◁	Glass beads	700	0.025	tube bundle
	◪	Quartz sand	720	0.025	
	▬	Aluminum	750	0.025	
Vakhrushev *et al.* [19]	▼	Coke	430	0.025	903
Tischchenko and Khvastukhin [23]	▽	High alumina	970–1450	0.036	1273–1373
Lese and Kermode [24]	◈	Glass beads	295	0.0286	Room temperature

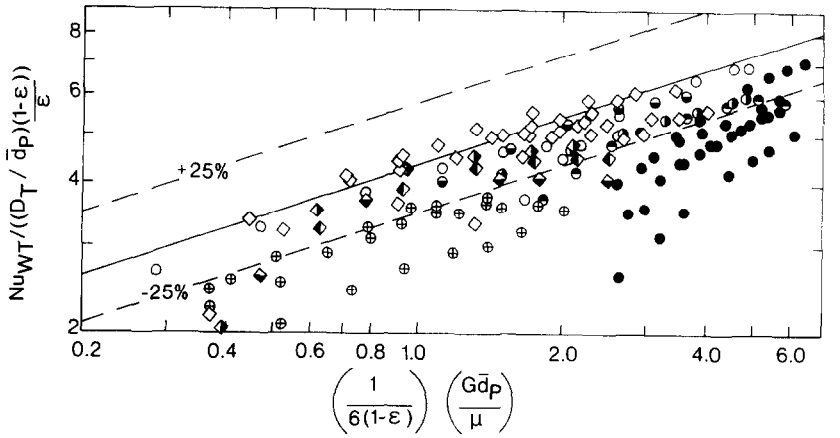

FIG. 9. Comparison of present experimental data with the correlation of Gelperin *et al.* [16]. Symbols and related details are explained in Table 3.

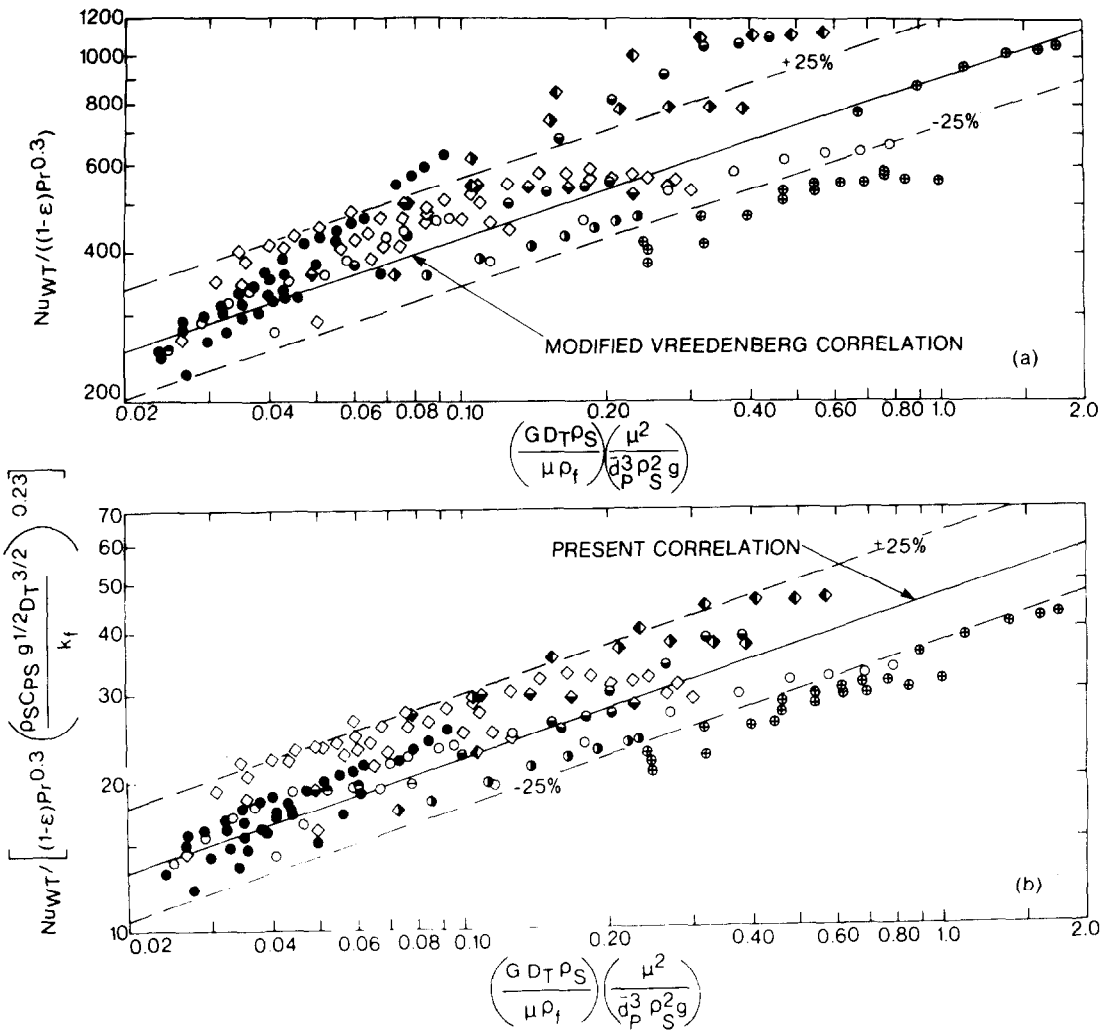

FIG. 14. Comparison of present experimental data with (a) modified Vreedenberg's correlation [15] and (b) present correlation. Symbols and related details are explained in Table 3.

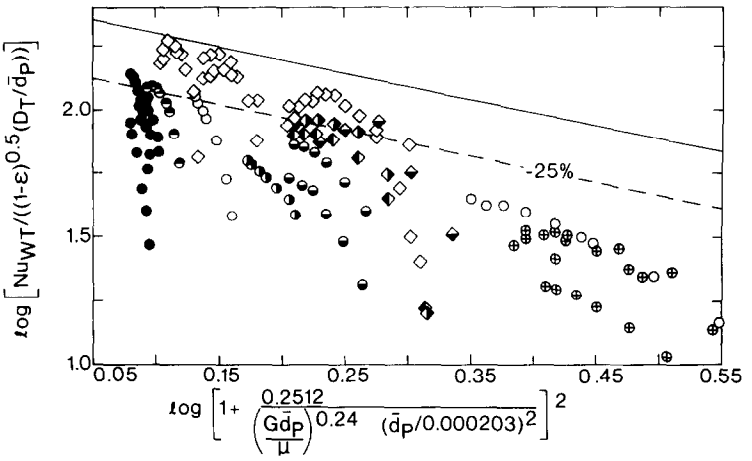

FIG. 12. Comparison of present experimental data with the correlation of Genetti *et al.* [17]. Symbols and related details are explained in Table 3.

As shown in Fig. 14(b), the predicted values of h_w are within $\pm 25\%$ of the present experimental results for all the solid particles except for silica sand ($\bar{d}_p = 167\,\mu$m).

4.3. *Comparison with earlier studies*

The reliability of a correlation is considerably enhanced if it can also predict the data not employed in its development. We have, therefore, undertaken here a detailed comparison between the predictions from the present correlation and the data of various investigators. This is graphically displayed in Figs. 15 and 16. The values of ε can be calculated from equation (7) if the sphericity of solid particles, ϕ_s, is known. For all other cases the correlation of Goroshko *et al.* [40] is used. All the necessary properties of air are calculated at the average of the bed and tube surface temperatures. In general, there is a good agreement between the predicted values of h_w from the present correlation and the experimental values of h_w of various investigators. However, the experimental values of h_w of Cherrington *et al.* [32] are consistently larger than the calculated values of h_w. This discrepancy can be partially explained by examining the method employed for the determination of h_w. Cherrington *et al.* [32] measured the local heat transfer coefficient by placing small electrically heated strips along the circumference of an unheated Plexiglas tube. The average heat transfer coefficient, h_w, was then obtained by the integration of the experimental values of the local heat transfer coefficients over the tube circumference. Since the Plexiglas tube was not heated, the measured heat transfer coefficient would be too large, because the solid particles moving along the surface of the tube would not be preheated before reaching the heated strip. The amount of preheating of particles before reaching a corresponding position when the whole of the tube is heated would depend on factors such as tube diameter, physical and thermal properties of solid particles, and mass fluidizing velocity. The

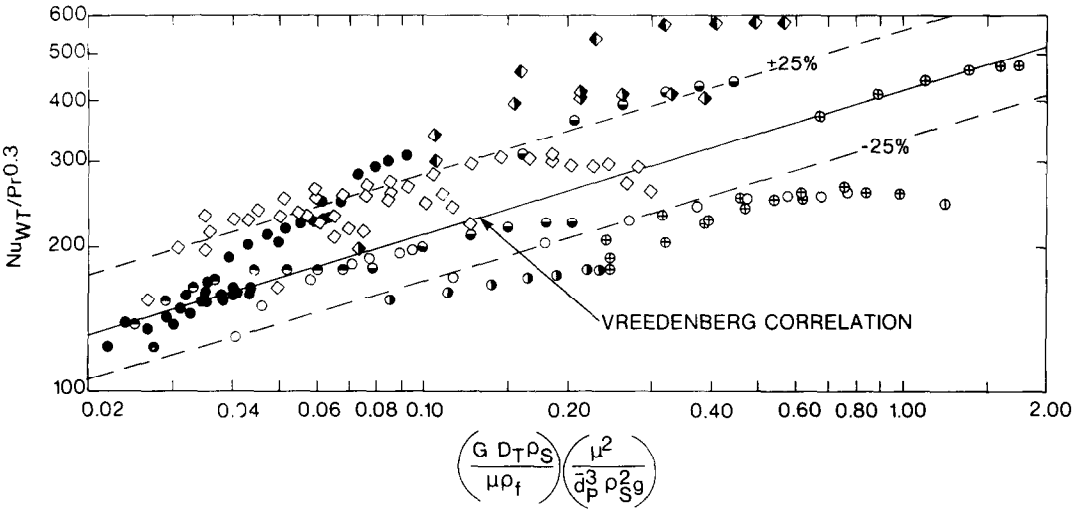

FIG. 13. Comparison of present experimental data with the Vreedenberg's correlation [11]. Symbols and related details are explained in Table 3.

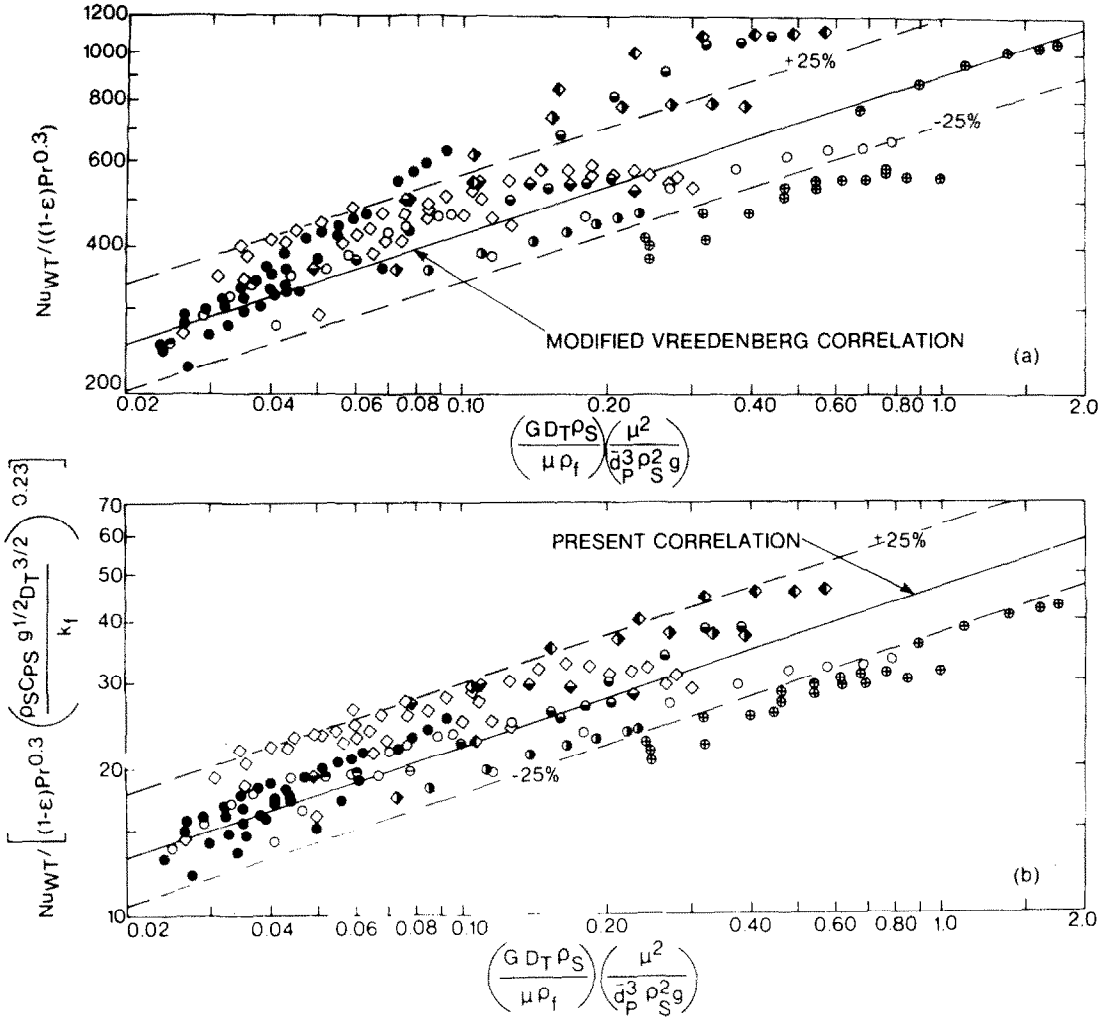

FIG. 14. Comparison of present experimental data with (a) modified Vreedenberg's correlation [15] and (b) present correlation. Symbols and related details are explained in Table 3.

agreement between the experimental values of Vreedenberg [11] for $D_T = 33.6$ mm at low values of fluidizing velocity and the predictions based on the correlation of equation (8) is not good.

5. SUMMARY AND CONCLUSIONS

Based on this experimental study and calculations from different correlations the following conclusions may be drawn:

(1) None of the existing correlations for h_w are capable of predicting the present data taken under different experimental conditions.
(2) The correlation of equation (8) for h_w which also accounts for the volumetric heat capacity of the solid particles is found to yield good agreement for all the present data and the data of the other investigators.

REFERENCES

1. N. S. Grewal, Ph.D. Thesis, Experimental and theoretical investigations of heat transfer between a gas–solid fluidized bed and immersed tubes, University of Illinois at Chicago Circle (1979).
2. S. S. Zabrodsky, N. V. Antonishin and A. L. Parnas, On fluidized bed-to-surface heat transfer, *Can. J. Chem. Engng* **54**, 52–57 (1976).
3. J. S. M. Botterill, *Fluid-Bed Heat Transfer*. Academic Press, New York (1975).
4. C. Gutfinger and N. Abuef, In *Advances in Heat Transfer*, Vol. 10, pp. 167–218, edited by T. F. Irvine, Jr. and J. P. Hartnett. Academic Press, New York (1974).
5. S. S. Zabrodsky, *Hydrodynamics and Heat Transfer in Fluidized Beds*, MIT Press, Cambridge, Massachusetts (1966).
6. N. I. Gelperin and V. G. Einshtein, In *Fluidization*, pp. 517–540, edited by J. F. Davidson and D. Harrison. Academic Press, New York (1971).
7. D. Kunii and O. Levenspiel, *Fluidization Engineering*, pp. 265–301, Wiley, New York (1969).

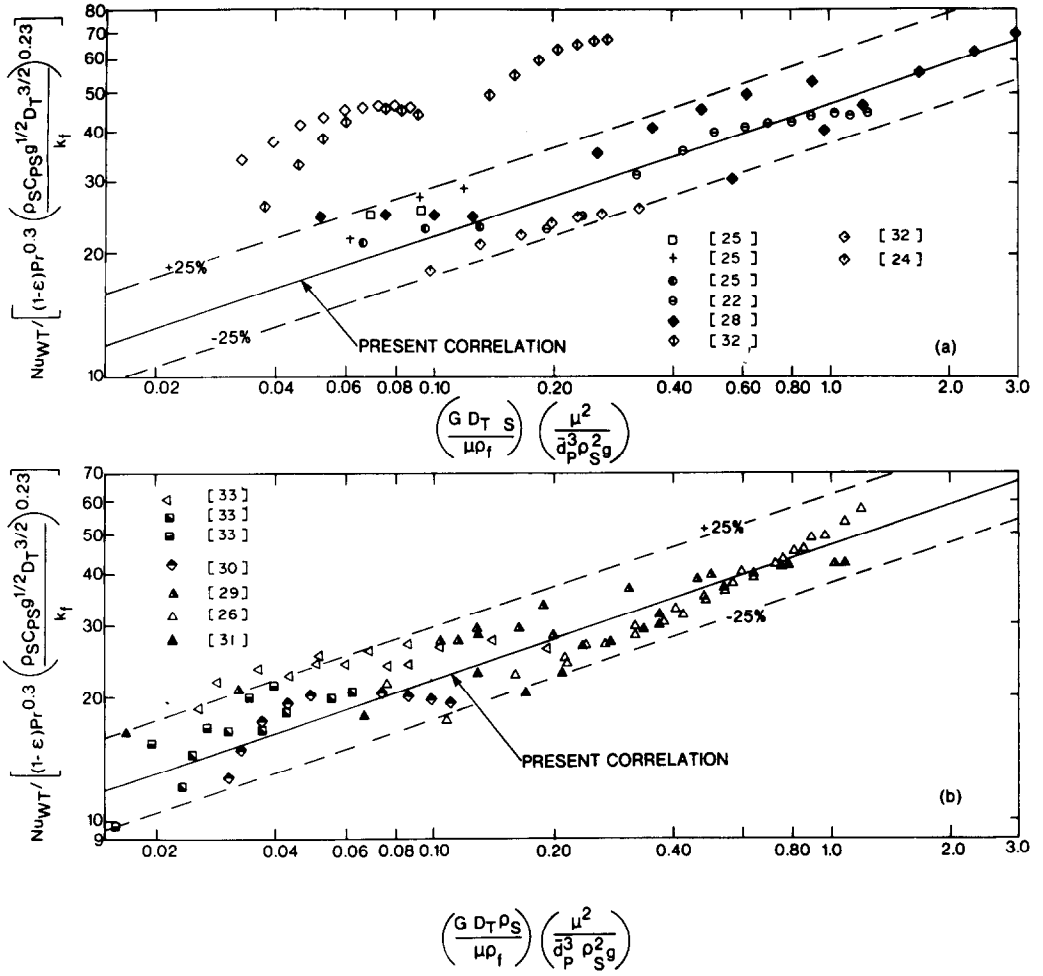

FIG. 15. Comparison of experimental data of various investigators with the present correlation. Symbols and related details are explained in Table 3.

8. F. A. Zenz and D. F. Othmer, *Fluidization and Fluid–Particle Systems*, pp. 421–462, Van Nostrand-Reinhold, Princeton, New Jersey (1960).
9. M. Leva, *Fluidization*, McGraw-Hill, New York (1959).
10. S. C. Saxena, N. S. Grewal, J. D. Gabor, S. S. Zabrodsky and D. M. Galershtein, In *Advances in Heat Transfer*, Vol. 14, pp. 149–247, edited by T. F. Irvine, Jr and J. P. Hartnett, Academic Press, New York (1978).
11. H. A. Vreedenberg, Heat transfer between a fluidized bed and a horizontal tube, *Chem. Engng Sci.* **9**, 52–60 (1958).
12. A. N. Ternovskaya and Yu. G. Korenberg, *Pyrite Kilning in a Fluidized Bed*, Izd. Khimiya, Moscow (1971).
13. J. C. Petrie, W. A. Freeby and J. A. Buckham, In-bed heat exchangers, *Chem. Engng. Prog. Symp. Ser.* **64**(67), 45–51 (1968).
14. V. G. Ainshtein, An investigation of heat transfer process between fluidized beds and single tubes submerged in the bed, in *Hydrodynamics and Heat Transfer in Fluidized Beds*, pp. 270–272, edited by S. S. Zabrodsky, M.I.T. Press, Cambridge, Massachusetts (1966).
15. B. R. Andeen and L. R. Glicksman, Heat transfer to horizontal tubes in shallow fluidized beds, *ASME — A. I. Ch. E. Heat Transfer Conference*, Paper No. 76-HT-67, St. Louis, MO, August 9–11 (1976).
16. N. I. Gelperin, V. Ya. Kruglikov and V. G. Ainshtein, In Heat transfer between a fluidized bed and a surface, by V. G. Ainshtein and N. I. Gelperin, *Int. Chem. Engng* **6**(1), 67–73 (1966).
17. W. E. Genetti, R. A. Schmall and E. S. Grimmett, The effect of tube orientation on heat transfer with bare and finned tubes in a fluidized bed, *Chem. Engng Prog. Symp. Ser.* **67**(116), 90–96 (1971).
18. K. Janssen, Dr. Ing. Thesis, Aachen (1973).
19. I. A. Vakhrushev, Ya. A. Botnikov and N. G. Zenchenkov, Heat transfer from a fluidized bed of hot coke to the surface of horizontal tubes, *Int. Chem. Engng* **3**(2), 207–210 (1963).
20. H. J. Natusch and H. Blenke, Wärmeübertragung and Rippenrohren in Gas-Fliesbetten, Verfahrenstechnik, *Chemie-Ingr-Tech.* **7**(10), 293–296 (1973).
21. V. G. Ainshtein and N. I. Gelperin, Heat transfer between a fluidized bed and a surface, *Int. Chem Engng* **6**(1), 67–74 (1966).
22. J. C. Chen, Heat transfer to tubes in fluidized beds, *ASME — A. I. Ch. E. Heat Transfer Conf. 1976*, Paper 76-HT-75 (1976).

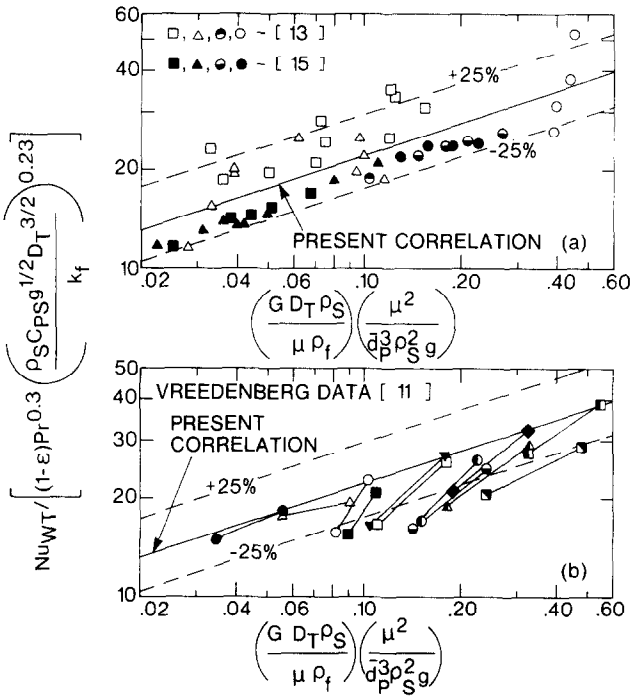

FIG. 16. Comparison of experimental data of other investigators with the present correlation.

23. A. T. Tishchenko and Yu. I. Khvastukhin, *Fluidized Bed Furnaces and Heat Exchangers*, Naukova Dumka, Kiev (1973).
24. H. K. Lese and R. I. Kermode, Heat transfer from a horizontal tube to a fluidized bed in the presence of unheated tubes, *Can. J. Chem. Engng* **50**, 44–48 (1972).
25. E. N. Ziegler, Heat and mass transfer to a gas-fluidized bed of solid particles, Argonne National Laboratory Report No. 6807 (1963).
26. N. V. Antonshin, In *Hydrodynamics and Heat Transfer in Fluidized Beds*, pp. 270–272, by S. S. Zabrodsky, M.I.T. Press, Cambridge, MA (1966).
27. N. I. Gelperin, V. G. Einstein and N. A. Romanova, *Khim. Mashinostr. No. 5*, 13 (1963), in *Fluidization*, p. 489, edited by J. F. Davidson and D. Harrison, Academic Press, New York (1971).
28. W. J. Bartel and W. E. Genetti, Heat transfer from a horizontal bundle of bare and finned tubes in an air fluidized bed, *Chem. Engng Prog. Symp. Ser.* **69**(128), 85–93 (1973).
29. N. I. Gelperin, V. G. Ainshtein and A. V. Zaikovskii, Variation of heat transfer intensity around the perimeter of horizontal tube in a fluidized bed, *J. Engng Phys.* **10**(6), 473–475 (1966).
30. R. Noack, Lokaler Wärmeübergang an horizontalen Rohren in Wirbelschichten, *Chemie- Ingr- Tech.* **42**(6), 371–376 (1970).
31. W. C. Howe and C. Aulisio, Control variables in fluidized bed steam generation, *Chem. Engng Prog.* **73**(7), 69–73 (1977).
32. D. C. Cherrington, L. P. Golan and F. G. Hammitt, Industrial application of fluidized bed combustion — single tube heat transfer studies, *Proceedings of the Fifth International Conference on Fluidized Bed Combustion*, Washington, DC (1977).
33. B. Neukirchen and H. Blenke, Gestaltung horizontaler Rohrbundel in Gas-Wirbelschichtreaktoren nach Wärmetechnischen, *Chemie-Ingr-Tech.* **45**(5), 307–312 (1973).
34. S. J. Priebe and W. E. Genetti, Heat transfer from a horizontal bundle of extended surface tubes to an air fluidized bed, *Chem. Engng Prog. Symp. Ser.* **73**, No. 161, 38–43 (1977).
35. N. S. Grewal and S. C. Saxena, Investigations of heat transfer from immersed tubes in a fluidized bed, *Fourth National Heat Mass Transfer Conference*, India, pp. 53–58 (1977).
36. N. S. Grewal and S. C. Saxena, Effect of surface roughness on heat transfer from horizontal immersed tubes in fluidized bed, *Trans. Am. Inst. Mech. Engrs, J. Heat Transfer* **101**, 397–403 (1979).
37. N. S. Grewal, S. C. Saxena, A. F. Dolidovich and S. S. Zabrodsky, Effect of distributor design on heat transfer from an immersed horizontal tube in a fluidized bed, *Chem. Engng J.* **18**, 197–201 (1979).
38. S. C. Saxena and G. J. Vogel, The measurement of incipient fluidization velocities in a bed of coarse dolomite at temperature and pressure, *Trans. Inst. Chem. Engrs* **55**, 184–189 (1977).
39. E. N. Ziegler, L. B. Koppel and W. T. Brazelton, Effects of solid thermal properties on heat transfer to gas fluidized beds, *I/EC Fundamentals* **3**(4), 324–329 (1964).
40. V. D. Goroshko, R. B. Rozenbaum and O. M. Todes, Approximate hydraulic relationships for suspended beds and hindered fall, *Izv. Vuzov, Neft' i Gaz, No. 1*, 125–131 (1958), in *Hydrodynamics and Heat Transfer in Fluidized Beds*, pp. 71–73, by S. S. Zabrodsky, M.I.T. Press. Cambridge, MA (1966).

TRANSFERT THERMIQUE ENTRE UN TUBE HORIZONTAL ET UN LIT FLUIDISE GAZ–SOLIDE

Résumé—Des expériences sont faites pour mesurer le coefficient de transfert thermique entre un tube horizontal chauffé électriquement et des lits fluidisés air–solide avec des particules de verre, dolomite, sable, carbure de silice et alumine. On étudie les effets de la dimension de la particule, de la forme, de la densité et de la chaleur massique ainsi que de la vitesse de l'air, de la dimension du tube, de sa nature, de la hauteur du lit, du dessin du distributeur. Des résultats expérimentaux sur le coefficient de transfert thermique h_w sont comparés avec les formules déja existantes. Ces formules sont trouvées ne pas reproduire les données présentes. Une formule est proposée pour h_w, sur la base de ces expériences et elle est examinée à travers les données disponibles dans diverses publications.

WÄRMEÜBERGANG ZWISCHEN EINEM HORIZONTALEN ROHR UND EINEM GASDURCHSTRÖMTEN FLIEßBETT

Zusammenfassung—Es wurden Versuche durchgeführt, um den Wärmeübergangskoeffizienten zwischen einem elektrisch beheizten waagerechten Einzelrohr und einem von Luft durchströmten Fließbett aus Glaskugeln, Dolomit, Sand, Silikonkarbid und Aluminiumteilchen zu bestimmen. Folgen der Einflußgrößen auf den Wärmeübergang wurden untersucht: Teilchengröße, Gestalt Dichte und spezifische Wärme, Luftdurchsatz, Rohrabmessungen, Rohrwerkstoffe, Höhe des Fließbetts, Wärmestromdichte und Verteilerbauart. Die gemessenen Werte des Wärmeübergangskoeffizienten α wurden mit Werten verglichen, die nach bekannten Gleichungen berechnet wurden. Es wurde gefunden, daß diese Gleichungen die vorliegenden Daten unzulänglich wiedergeben. Deshalb wird eine Gleichung für α auf der Basis unserer Meßergebnisse vorgeschlagen und an Literaturwerten überprüft.

ТЕПЛООБМЕН МЕЖДУ ГОРИЗОНТАЛЬНОЙ ТРУБОЙ И СЛОЕМ ТВЕРДЫХ ЧАСТИЦ, ПСЕВДООЖИЖЕННЫХ ГАЗОМ

Аннотация — Проведены экспериментальные измерения коэффициента теплообмена между нагреваемой электрическим током горизонтальной трубой и слоями стеклянных шариков, частиц доломита, песка, карбида кремния и алюминия, псевдоожиженных газом. Исследовалось влияние размера, формы, плотности и теплоёмкости частиц, массовой скорости газа, размера и материала трубы, высоты слоя, плотности теплового потока и конструкции распределительной решетки на интенсивность теплообмена. Экспериментальные значения коэффициента теплообмена h_w сравниваются с расчетными, полученными с помощью известных корреляций. Показано, что последние не описывают адекватно экспериментальные данные. Поэтому для h_w предложено соотношение, полученное на основе данных экспериментов, которое удовлетворительно описывает и имеющиеся в литературе данные.